air was passed over the solution, out through the condenser, and into standard barium hydroxide. By using a fritted glass bubbler it was found possible to use but one trap, however the fritted glass face must be turned downward or the pores soon become clogged. After the air had been turned on, the solution was refluxed gently for 1.5 hours. The reflux condenser efficiently prevented the escape of the volatile acids as was shown by analyzing a test mixture containing known amounts of sodium carbonate, sodium acetate, and oxalic acid.

Ultraviolet absorption spectra of the water-soluble acids from ozonized coal, humic acids from air oxidized coal, and humic acids from carbon black were obtained with a Beckman quartz spectrophotometer. For this purpose, 0.1-g. samples were dissolved in 100 ml. of 0.1 *N* sodium hydroxide. Fused silica cells and slit widths of 0.2 to 1.9 mm. were used. Spectrograms were constructed as shown in Fig. 1.

STATE COLLEGE, PENNSYLVANIA

RECEIVED FEBRUARY 2, 1951

[CONTRIBUTION FROM THE RESEARCH AND DEVELOPMENT DEPARTMENT, PITTSBURGH COKE AND CHEMICAL COMPANY]

A Comparison of Pore Size Distributions of Activated Carbons Calculated from Nitrogen and Water Desorption Isotherms

BY A. J. JUHOLA, A. J. PALUMBO AND S. B. SMITH

Pore size distribution curves for several activated carbons computed by the Barrett, Joyner, Halenda method from the low temperature nitrogen desorption isotherms were compared with pore size distribution curves computed from water desorption isotherms by the method described by Juhola and Wiig. A semi-quantitative agreement was found between the distribution curves computed by the two methods for pores in the 22 to 300 Å. radius range. Below 22 A. radius the method based on nitrogen absorption is not theoretically applicable. The water adsorption method was found to be theoretically applicable to the complete gamut of pores found in activated carbons and the method yielded distribution curves from which surface areas were computed that were in essential agreement with the Brunauer, Emmett and Teller (BET) areas.

In a recent publication Barrett, Joyner and Halenda[1] described a method for computing the pore size distributions of various types of porous adsorbents from nitrogen adsorption data determined at liquid nitrogen temperature. This technique was developed to deal with relatively coarsely porous adsorbents, such as some clay cracking catalysts, bone chars and silica gel. In their computations, it was assumed that equilibrium between the gas phase and the adsorbed phase (liquid state) during desorption was determined by two mechanisms: (1) physical adsorption in multi-layers on the pore walls, and (2) condensation in capillaries. The pore radius corresponding to a specified relative vapor pressure on the desorption isotherm was the thickness, t, of the physically adsorbed layer plus the meniscus radius, r_K, of the condensed phase in the inner capillary. To get the relationship between t and P/P_0, they used the experimental data of Shull,[2] determined on a non-porous crystalline material, assuming that the same relationship applied to porous materials. The capillary radius, as a function of P/P_0, was expressed by the classical Kelvin equation

$$r_K = \frac{2\sigma V \cos\theta}{RT \ln P_0/P}$$

Here σ is the surface tension and V the molar volume of the liquid adsorbate, θ, the contact angle, which is assumed to be zero for nitrogen, and P/P_0 the relative vapor pressure.

In an earlier publication, Juhola and Wiig[3] described a method for computing the pore size distributions of activated carbons from the desorption side of the water adsorption isotherms determined at room temperature. In this case the pore radius corresponding to any P/P_0 was given directly by the Kelvin equation, since it was believed that the formation of any physically adsorbed layer on the pore walls was negligible. This method is limited because it is applicable only to activated carbons which do not possess hydrophilic groups on the surface.

In this paper a comparison is made between these two methods of computing pore size distributions as applied to activated carbons. Since both methods (although based on considerably different adsorption theories) should give the same pore size distribution for a given carbon, the agreement or disagreement serves to confirm the validity, and/or to indicate the weaknesses of the methods.

Experimental

The nitrogen adsorption–desorption isotherms were determined at liquid nitrogen temperature in a conventional volumetric apparatus of the type used by Brunauer and Emmett.[4]

The apparatus and procedure used in determining the water adsorption–desorption isotherms, except for small modifications, were described in the paper by Juhola and Wiig.[3] The weight of water adsorbed on the carbon was determined gravimetrically following each adsorption or desorption, after allowing a suitable length of time (1 to 2 hours) for the system to attain equilibrium. These measurements were made at 25°.

According to previous water adsorption studies on activated carbons,[3] $\cos\theta$ (in the Kelvin equation) was found to be 0.49 giving a contact angle of 60.6°. The molar volume, V, of the adsorbed water was in part a function of P/P_0. The best average V for several carbons investigated was 20 cc. This value was used in the Kelvin equation and in converting weight of adsorbed water to pore volume.

The carbon samples were evacuated at about 400° for 1 to 2 hours prior to the adsorption experiments. For each carbon the same sample was used in each gas adsorption measurement.

Results and Discussion

The experimental results on four activated carbons, representing rather widely differing types of pore structures, are presented in these comparisons. Some physical data which are intended

(1) Elliott P. Barrett, Leslie G. Joyner and Paul P. Halenda, THIS JOURNAL, **73**, 373 (1951).

(2) C. G. Shull, *ibid.*, **70**, 1405 (1948).

(3) A. J. Juhola and E. O. Wiig, *ibid.*, **71**, 2069 (1949).

(4) P. H. Emmett and S. Brunauer, *ibid.*, **59**, 1553 (1937); S. Brunauer and P. H. Emmett, *ibid.*, **59**, 2682 (1937).

to give some indication of the diversity of these carbons are given in Table I.

TABLE I

DENSITIES, PORE VOLUMES AND SURFACE AREAS OF ACTIVATED CARBON

Carbon	Bulk density, g./cc.	Total pore, vol., cc./g.	Vol. of pores of radii less than 300 Å., cc./g.	BET[5] surface area, m.²/g.
B 334-3C	0.192	3.504	2.750	1405
RB (12-30)	.380	1.217	0.770	1325
CXA (4-6)	.476	1.027	.535	1178
Darco (12-20)	.420	0.962	.725	612

The first carbon, B 334-3C is an experimental sample. The other three are commercial carbons; RB (12-30 mesh) is prepared by the Pittsburgh Coke & Chemical Co., Pittsburgh, Pa., CXA (4–6 mesh) is a Columbia carbon prepared by the Carbide & Carbon Chemical Corp., New York, N. Y., and the last is one of the granular carbons produced by the Darco Corp., New York, N. Y.

Adsorption (desorption) isotherms of the two vapors for three of the carbons investigated are plotted in Figs. 1 and 2. In general, the characteristic difference between the nitrogen and water adsorption isotherms for activated carbons is that nitrogen is adsorbed at low P/P_0 while water adsorption generally becomes appreciable at P/P_0 greater than 0.4. According to adsorption theories which form the basis of the two methods of pore size computations, the nitrogen adsorption at low P/P_0 is governed by the magnitude of the surface area, while for water the lower P/P_0 limit at which appreciable adsorption begins is governed by the diameter of the smallest pores.

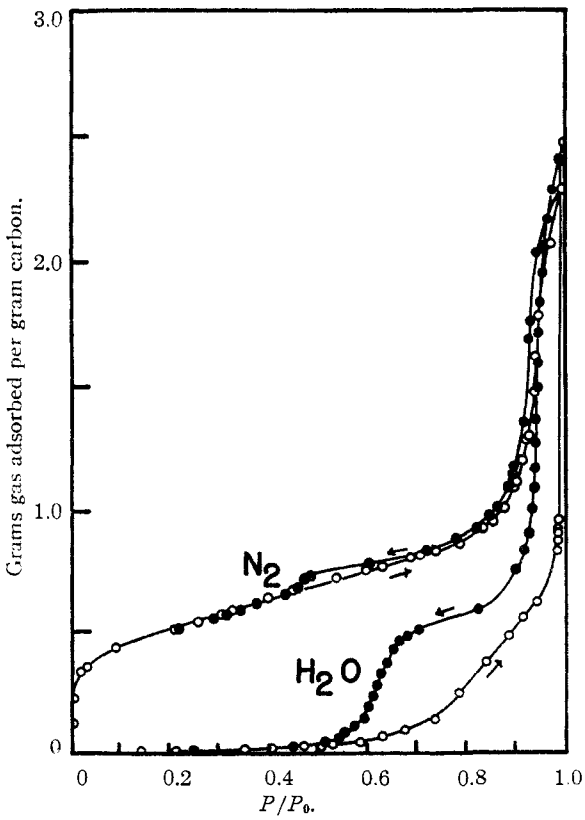

Fig. 1.—Adsorption isotherms of nitrogen at −195.8° and water at 25°; exp. carbon B334-3C.

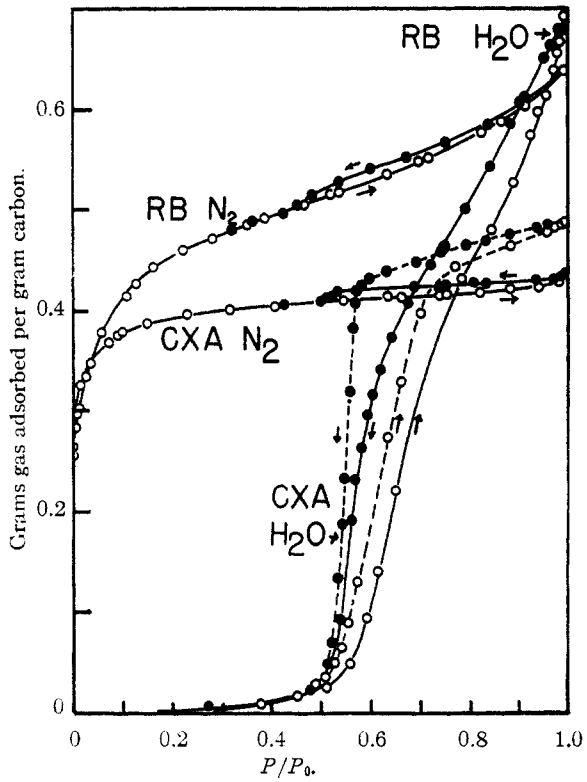

Fig. 2.—Adsorption isotherms of nitrogen at −195.8° and water at 25°; PCC RB and Columbia CXA.

On activated carbons having hydrophilic groups on the surface, water adsorption does not always occur by straight capillary condensation but a considerable amount may be taken up by physical or chemisorption on the surface. Adsorption of this type becomes evident when the moisture pick-up is relatively large at P/P_0 approaching zero and the two branches of the hysteresis loop do not unite, as for example, in the water adsorption in Fig. 3. If the Kelvin equation is applied to a water desorption isotherm of this type, it will give a misleading distribution curve, especially in the small pore end.

Although the desorption isotherms of these two vapors are different, the pore size distribution curves, Figs. 4 and 5, computed from them are similar for each carbon. For carbon B 334-3C, Fig. 4, both curves show small pore volume in the pore radius ranges 20 to 70 Å. and 180 to about 400 Å. In the radius range 70 to 180 Å., the radii by the nitrogen desorption method are larger, being 145 Å. at the mid-point of the range as compared to 105 Å. by the water desorption method. The two curves in this region may be brought into closer agreement if cos θ for the adsorbed water is increased from 0.49 to 0.62 and the molar volume, V, increased from 20 to 21. Adjustments in cos θ in this direction are sometimes justifiable because θ is sensitive to the chemical nature of the surface. If B 334-3C is more hydrophilic than the carbons

(5) S. Brunauer, P. H. Emmett and E. Teller, THIS JOURNAL, 60, 309 (1938).

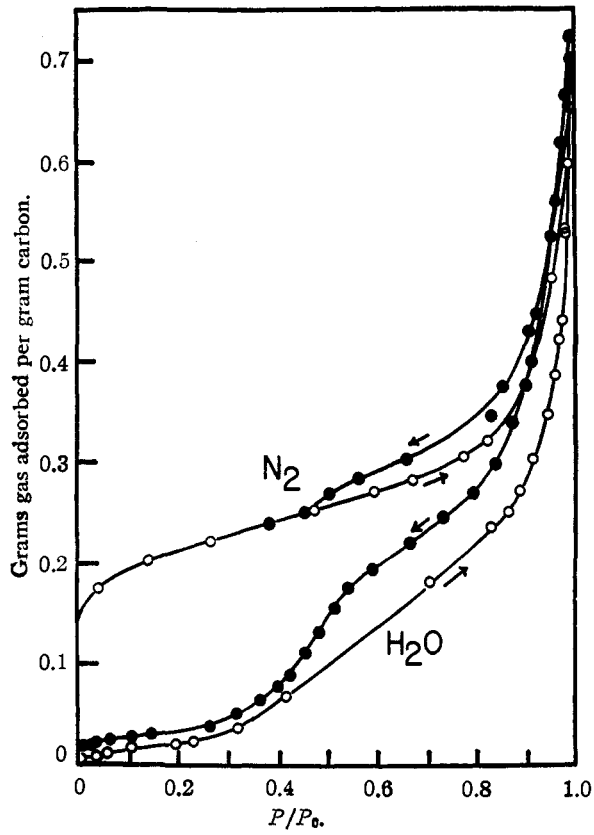

Fig. 3.—Adsorption isotherms of nitrogen at −195.8° and water at 25°; Darco carbon.

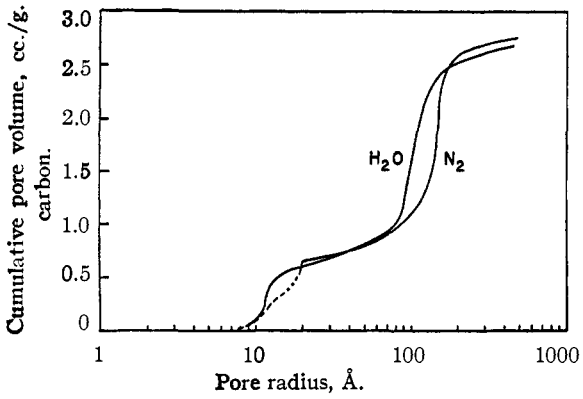

Fig. 4.—Pore size distribution curves computed from nitrogen and water desorption isotherms; experimental carbon B334-3C.

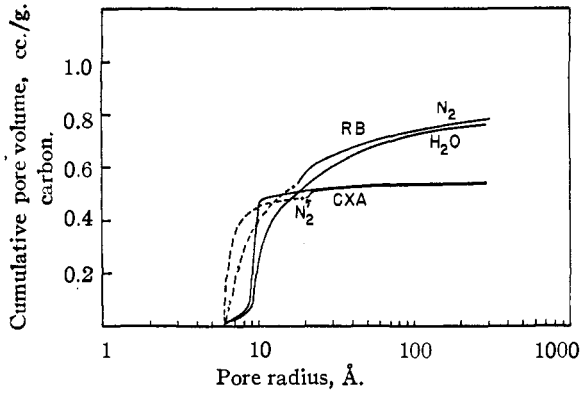

Fig. 5.—Pore size distribution curves computed from nitrogen and water desorption isotherms.

used in the previous studies[3] when the value 0.49 was determined for cos θ, then cos θ in this case could be greater than 0.49. No justification can be given for any increase in V at the present time.

The carbon B 334-3C is unusual in its large pore volume in the 70 to 180 Å. pore radius range as the typical carbon is more like RB or CXA, with a fairly small volume of pores in this region. CXA possesses practically no pores, only 0.03 cc., in the radius range 23 to 300 Å.; for RB the volume is greater being about 0.18 cc. For both carbons the agreement between the two methods is quite satisfactory in this radius range.

In the small radius range, 8 to 20 Å., the pore size distribution is in a region where the method based on the nitrogen desorption is no longer theoretically applicable. It is generally believed that at the P/P_0 where the adsorption and desorption branches of the hysteresis loop join, capillary condensation ceases and at lower P/P_0 the adsorption is primarily unimolecular. For B 334-3C and RB the P/P_0 at the point of hysteresis inception is 0.45, which according to the Barrett–Joyner calculations correspond to a pore radius of 18.1 Å. For CXA the point of inception is 0.49 P/P_0 and the corresponding pore radius 20 Å. For this reason the continuation of the distribution curves below 18 or 20 Å. were put in with dotted lines to show that they are without theoretical basis.

At 0.45 P/P_0 the inner capillary radius, r_K, is 11.7 which is equivalent to 2.7 molecular diameters. In this estimate, 4.32 Å. is used as the nitrogen molecular diameter calculated from the liquid molar volume assuming spherical molecules and closest hexagonal packing. The thickness, t, of the physically adsorbed layer is 6.5 Å. which is equivalent to 1.5 nitrogen molecular diameters.

It follows from the above interpretation of theory and estimates of adsorbed layer thickness that at about 0.45 P/P_0 the desorption process has reached the end of a range of P/P_0 in which the inner capillary phase has become increasingly unstable, and at this point only a physically adsorbed layer is left on the pore walls that is statistically 1.5 molecular diameters in thickness. By inspection of the nitrogen desorption isotherms in Figs. 1 and 2, it is apparent that this unstable period begins at about 0.54 P/P_0, *i.e.*, at 22 Å. pore radius. The liquid volume of nitrogen desorbed from 0.54 P/P_0 to 0.45 P/P_0, or to 0.49 P/P_0 for CXA, is then the volume of the inner capillaries of pores 22 Å. and less in radius. For B 334-3C, this volume is 0.10 cc./g., for RB, 0.06 cc/g. and for CXA, 0.03 cc./g. In these computations the normal density, 0.808 g./cc. for liquid nitrogen was used.

These inner capillary volumes of pores 22 Å. and less in radius were also computed for the three carbons from the pore size distribution curves determined from the water desorption data. In these computations the pore size distribution was treated as a series of cylindrical segments (of volume Δv) of increasing average radius, $\bar{r}_p$, from 6 to 22 Å. From $\bar{r}_p$, 6.5 Å. was subtracted to give the inner capillary radius $\bar{r}_c$. The inner capillary

volume increment Δv_c is then related to Δv by the equation

$$\Delta v_c = \left(\frac{\bar{r}_c}{\bar{r}_p}\right)^2 \Delta v$$

By summing up the Δv_c over the radius range 6 to 22 Å. one obtains the inner capillary volume. (As an example, the steps of the computation for B 334-3C are given in Table II.)

TABLE II

CALCULATION OF INNER CAPILLARY VOLUME OF PORES 22 Å. AND LESS IN RADIUS FOR CARBON B 334-3C

Total inner capillary volume—0.126 cc./g.

Δv, cc./g.	Radius interval, Å.	$\bar{r}_p$, Å.	$\bar{r}_p$ − 6.5	Δv_c, cc./g.	$\Sigma \Delta v_c$ cc./g.
0 −0.05	6 - 8.8	7.5	1.0	...	...
.05- .10	8.8-10.0	9.4	2.9	0.005	0.005
.10- .15	10.0-10.7	10.4	3.9	.007	.012
.15- .20	10.7-11.1	10.9	4.4	.008	.020
.20- .25	11.1-11.3	11.2	4.7	.009	.029
.25- .30	11.3-11.5	11.4	4.9	.009	.038
.30- .35	11.5-11.8	11.6	5.1	.010	.048
.45- .40	11.8-12.3	12.0	5.5	.010	.058
.40- .45	12.3-13.0	12.6	6.1	.012	.070
.45- .50	13.0-14.2	13.6	7.1	.014	.084
.50- .55	14.2-16.0	15.1	8.6	.016	.100
.55- .60	16.0-10.5	18.2	11.7	.021	.121
.60- .61	20.5-22.0	21.2	14.7	.005	.126

For B 334-3C the computed inner capillary volume is 0.126 cc./g., for RB, 0.09 cc./g. and for CXA, 0.05 cc./g. These volumes are 0.02 to 0.03 cc./g. larger than those measured from the isotherms. This may be expected since no correction was made for packing effects in the isothermal volume measurement. When molecules are packed into small pores of the radius dealt with here, the volume occupied by the molecules is greater than that calculated from the weight of nitrogen using the normal density (0.808 g./cc.).

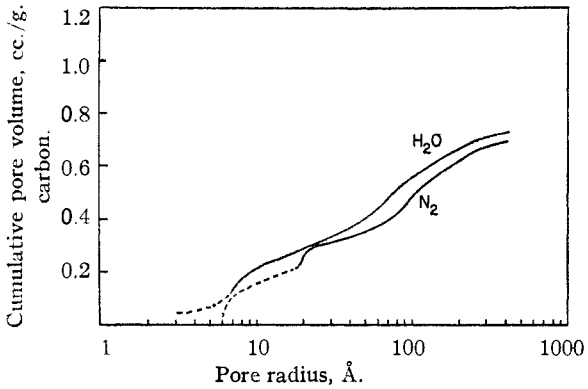

Fig. 6.—Pore size distribution curves computed from nitrogen and water desorption isotherms; Darco (12-20) carbon.

In Fig. 6 are shown the pore size distribution curves for the Darco carbon. The curve computed from the water adsorption data is shifted toward the small pore radii due to the hydrophilic nature of the surface. At the small pore end the curve trails off to radii which are obviously too small. The curve computed from the nitrogen adsorption data for pores greater than 22 Å. radius in this case is the more reliable one.

Calculation of Surface Area from Pore Size Distribution Curves.—The surface area may be calculated from the pore size distribution curve by summing up over the entire distribution curve increments of area ΔA associated with increments of volume Δv having average radii $\bar{r}_p$. Assuming cylindrical pore segments, the relationship between ΔA, Δv and r_p is

$$\Delta A = \frac{2\Delta v}{\bar{r}_p} \times 10^4$$

when ΔA is in square meters, Δv in cc. and $\bar{r}_p$ in Å.

In Table III the surface areas as calculated from the pore size distribution curves determined from the water isotherm are listed for comparison with the BET areas. Since the nitrogen adsorption method does not yield a valid distribution curve of pores below 18 Å. or possibly 22 Å. in radius, a total surface area calculation was not possible. Neither method yielded a complete and valid distribution curve for the Darco carbon. Where the water adsorption method was applicable it yielded areas that were in satisfactory agreement with BET areas.

TABLE III

SURFACE AREAS OF ACTIVATED CARBONS CALCULATED FROM PORE SIZE DISTRIBUTION CURVES AND BY THE BET METHOD

Carbon	BET[6] surface area, m.²/g.	H_2O pore size distribution curve, m.²/g.
B 334-3C	1405	1537
RB (12-30)	1325	1142
CXA (4-6)	1178	1114

PITTSBURGH, PENNA. RECEIVED JANUARY 8, 1951